COMMUNICATION

One step up in antiproliferative activity: the Ru-Zn complex [RuCp(PPh$_3$)$_2$-*μ*-dmoPTA-1κ*P*:2k^2*N,N'*-ZnCl$_2$](CF$_3$SO$_3$)

Zenaida Mendoza,[a] Pablo Lorenzo-Luis,[a] Franco Scalambra,[b] José M. Padrón[c] and Antonio Romerosa*[b]

Abstract: The synthesis, characterization and antiproliferative activity of the bis-metallic Ru-Zn complex [RuCp(PPh$_3$)$_2$-*μ*-dmoPTA-1κ*P*:2k^2*N,N'*-ZnCl$_2$](CF$_3$SO$_3$) (**4**) and the monometallic Ru complex [RuCp(PPh$_3$)$_2$(dmoPTA-1κ*P*)](CF$_3$SO$_3$) (**5**) are presented. Against human lung, cervix, breast, and colon solid tumour cell lines, the complex **4** showed an enhanced antiproliferative activity (GI$_{50}$ = 30-83 nM) when compared to its parent complex [RuCp(PPh$_3$)$_2$(HdmoPTA-1κ*P*)](CF$_3$SO$_3$) (**2**). Additionally, it was significantly more active against the breast cancer cell line T-47D than its sibling cobalt complex [RuCp(PPh$_3$)$_2$-*μ*-dmoPTA-1κ*P*:2κ^2*N,N'*-CoCl$_2$](CF$_3$SO$_3$) (**3**). When evaluated against non-tumour human cell line BJ-hTert the complex **4** showed to be 3-8 times less active, indicating a large selectivity against tumour cell, while compound **5** resulted not selective.

Introduction

Ruthenium(II)-based complexes have emerged as promising antitumor and antimetastatic agents with potential uses in platinum(II)-resistant tumours. In fact, some of them have shown broad diversity, in terms of activity, toxicity, and mechanisms of action due to a combination of chemical and biological properties.[1] Nevertheless, the platinum(II) complexes with antiproliferative properties show a similar ligand exchange kinetic than ruthenium(II)-anticancer drugs, which is crucial for displaying a significant anticancer activity.[2]

Stabilized Ru(II) complexes containing adequate ligands display the suitable redox and ligand-exchange properties needed to react with cancer cells. An accurate choice of the ligands coordinate to the metal could provide a selective antiproliferative activity of the formed complexes, killing the cancer cells selectively.[3,4] Additionally, the ligands are also useful for providing the optimal solubility for the complex both in water, the main component of living organism, and organic systems, such as the membrane cells. The hydrophilic/hydrophobic balance of a specie determines the *in vivo* behaviour and efficient under physiological conditions.[3b,4] The first report on the use of a water-soluble phosphine as ligand in developing anticancer ruthenium complexes dates back to 2011, when Dyson *et al.*, prepared a family of organometallic ruthenium compounds containing the hydrophilic phosphine 1,3,5-triaza-7-phosphaadamantane (PTA), which displayed significant anticancer activity towards different cancer cell lines, and particularly against platinum resistant cancer cells.[4b-d] Hydrolysis and the loss of one or more ligands are important processes in the mechanism of action of these water soluble ruthenium drugs due to increasing the number of potential targetable molecules.[1d,3-5] We have been interested in this field for years, firstly synthetizing and studying the family of water-soluble ruthenium complexes [RuCpX(L^1)(L^2)]$^{n+}$ (X = Cl; L^1 ,L^2 = PPh$_3$,PTA, mPTA, mTPPMS).[6] Later on we studied also the effect on the antiproliferative activity of the bis-N-methylated PTA *N,N'*-dimethyl-1,3,5-triaza-7-phosphaadamantane (dmPTA) and its derivative 3,7-H-3,7-dimethyl-1,3,7-triaza-5-phosphabicyclo[3.3.1]nonane (HdmoPTA).[7,8,9,10] This last ligand can be easily deprotonated and the resulting neutral 3,7-dimethyl-1,3,7-triaza-5-phosphabicyclo[3.3.1]nonane) (dmoPTA) is able to coordinate metals through the soft P and the two hard N$_{CH3}$ atoms, behaving in the latter case as a chelate.[11] The antiproliferative activity of the complex [RuCpCl(PPh$_3$)(HdmoPTA-1κ*P*)](CF$_3$SO$_3$) (**1**) (the so-called 1st generation) against colon cancer cells was significant better (GI$_{50}$ = 1.7 *μ*M) than that showed by cisplatin, that is currently used in anticancer therapy.[8] The substitution of the chloride in **1** by one PPh$_3$ led to complex [RuCp(PPh$_3$)$_2$(HdmoPTA-1κ*P*)](CF$_3$SO$_3$)$_2$·(**2**) (the so-called first member of the 2nd generation), which is more soluble in organic solvent, showing a substantial enhancement of the antiproliferative activity with respect to the starting complex **1**.[12] Elimination of the HdmoPTA-proton in **1** and further reaction with CoCl$_2$ provided the Ru-Co complex [RuCp(PPh$_3$)$_2$-*μ*-dmoPTA-1κ*P*:2κ^2*N,N'*-CoCl$_2$](CF$_3$SO$_3$) (**3**) (the second member of the 2nd generation), which showed a significant better antiproliferative activity than **1** (Figure 1), despite Co(II) is not particularly known for its antimetastatic properties.[13] The fact that the CoCl$_2$ is not an antiproliferative agent and that the antimetastatic activity of the Ru-Co complex is clearly and significantly better than the monometallic Ru starting complex led us to propose that complex **3** acts as a "Troyan Horse" that introduce both metals into the cell. To obtain a new example of this family of bimetallic complexes with possibly better antiproliferative activity but also amenable to be studied in dissolution by NMR, a diamagnetic metal should be coordinated to the dmoPTA-N$_{CH_3}$ atoms.

[a] PhD student Z. Mendoza, Prof. Dr. P. Lorenzo, Inorganic Chemistry Section, Chemistry Department, Universidad de La Laguna. C/Astrofísico Francisco Sánchez 2, 38206 La Laguna, Spain. E-mail: zeni_reni7@hotmail.com; plorenzo@ull.es

[b] Dr. F. Scalambra, Prof. Dr. A. Romerosa, Área de Química Inorgánica-CIESOL. Universidad de Almería, Carretera Sacramento s/n, Almería, Spain. E-mail: fs649@inlumine.ual.es; romerosa@ual.es.

[c] Prof. Dr. J. M. Padrón, BioLab, Instituto Universitario de Bio-Orgánica "Antonio González" (IUBO-AG). Universidad de La Laguna, C/Astrofísico Francisco Sánchez 2, 38206 La Laguna, E-mail: jmpadron@ull.es

Supporting information for this article is given via a link at the end of the document.

The hetero-metal selected was the diamagnetic Zn(II) that is an important component of some biological systems (i.e. as cytosolic Cu/Zn superoxide dismutase (SOD)).[14]

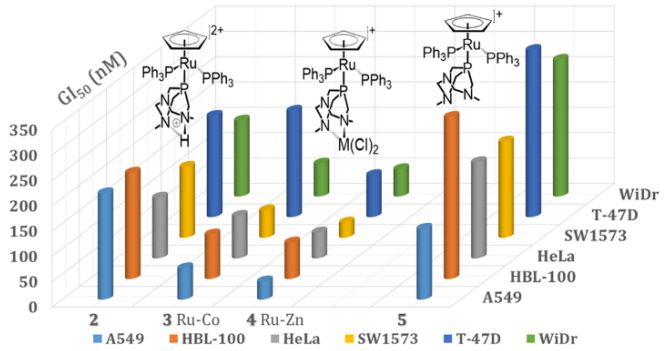

Figure 1. GI50 values (nM) for the 2nd generation ruthenium organometallic complexes against human solid tumor cells lines A549, HBL-100, HeLa, SW1573, T-47D and WiDr.

Results and Discussion

The Ru-Zn complex was initially synthetized by a procedure similar to that used for **3**,[13] by reaction of **2** with one equivalent of potassium tert-butoxide (*t*-BuOK) and further with one equivalent of $ZnCl_2$ in EtOH (Scheme 1, path *i*). This synthetic procedure is very sensitive to reaction conditions and a new one more robust is needed to obtain enough product to be studied. Pure deprotonated complex [RuCp(PPh_3)$_2$(dmoPTA-1κ*P*)](CF_3SO_3) (**5**) was synthetized by reaction of **2** with 1.1 equivalent of *t*-BuOK in THF (Scheme 1, path *ii*). The complex **5** is practically insoluble in water ($S_{25°C,H_2O}$ = 0.5 mg/mL) while it is significant soluble in a variety of organic solvents such as $CHCl_3$, THF, etc. This complex is stable in solution and solid state under N_2 for months but under air some evidences of decomposition ($^{31}P\{^1H\}$ NMR) are observed after one month in solid state and two days dissolved in $CHCl_3$. Reaction of **5** with $ZnCl_2$ in EtOH is a robust method to obtain the Ru-Zn complex (Scheme 1, path *iii*). The product was characterized by elemental analysis, IR and NMR spectroscopy as the expected bis-metallic Ru-Zn complex [RuCp(PPh_3)$_2$-*μ*-dmoPTA-1κ*P*:2κ^2*N,N'*-$ZnCl_2$](CF_3SO_3) (**4**).

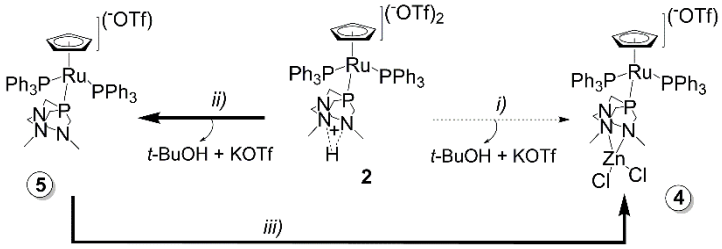

Scheme 1. Synthesis of **4**·and **5**; path *i)*: t-BuOK / EtOH / $ZnCl_2$, r.t.; *ii):* t-BuOK / THF, r.t. and *iii):* EtOH / $ZnCl_2$, r.t

The ^1H NMR of **4** was assigned by using ^1H-^1H COSY, ^1H-^{13}C HMBC and ^1H-^{13}C HSQC (see Figures S1-S6). The signals and chemical shift are those expected for the proposed complex composition in which the most interesting feature is the presence of two broad singlets, very close in chemical shift (2.15; 2.16 ppm), that could only be assigned to the N_{CH_3} groups. This shows that the methyl groups are chemically different. In contrast, the $^{13}C\{^1H\}$ NMR shows only a broad signal ascribable to both N_{CH_3}. Finally, the $^{31}P\{^1H\}$ NMR only showed the existence of one unique specie with phosphorus in dissolution with the expected signal pattern for the complex: a doublet for the PPh_3 ligand at 37.39 ppm and a triplet at -15.10 ppm due to the dmoPTA ($^2J_{PP}$ = 39.2 Hz). Both signals arise at similar chemical shift than those for starting complex **2** (38.44; -13.94 ppm) with similar coupling constant (39.4 Hz).[12] The single crystal X-ray diffraction structure of **4** showed that the asymmetric unit contains two OTf anions and two enantiomeric cationic Ru-Zn complexes (Figure 2, Table S1). The complex units are formed by the combination of the deprotonated moiety {RuCp(PPh_3)$_2$(dmoPTA-1κ*P*)}$^+$, which is similar to that in the starting complex, and one {$ZnCl_2$} moiety chelated to the N_{CH_3} atoms. The coordination sphere of the ruthenium atom displays a piano-stool geometry constituted by a η^5-Cp, two PPh_3 and a dmoPTA unit by its P atom (Figure 2). The Cp-ring is essentially planar with the larger separation from the overall-plan-Cp of only 0.0047 Å (C38) somewhat shorter than that in **2**·(0.0089 Å, C84) and **3**·(0.0079 Å, C39).[12,13] The Ru-$Cp_{centroid}$ distance (1.894 Å) is almost equivalent to that found for **2** and **3** (1.886 to 1.893 Å), and is similar to those found in other {RuCp}-complexes (from 1.836 to 1.929 Å; mean 1.893 Å).[15] The angle between the Cp-centroid plane and the P1–Ru1–P2 plane was found to be 46.6(1)°, which is virtually identical to that observed in **3** (46.9(9)°) but *ca.* 1.3° smaller than those found for **2**.[12,13] These values are considerably shorter than that found for complexes [RuClCp(PPh_3)-*μ*-dmoPTA-1κ*P*:2κ^2*N,N'*-MQ] (M = Co, Ni, Zn, Q = acac, Cl_2), which are in the range 53.7(2) - 56.85(0)° (average: 55.2°).[11b,c] The dihedral angles between the dmoPTA atoms vary from 52.4(5)-51.6(3) to 51.8(4)-52.7(4)° in agreement with those observed in related complexes [RuClCp(PPh_3)-*μ*-dmoPTA-1κ*P*:2κ^2*N,N'*-MCl_2] (M = Co, Ni, Zn) moiety (52.2(1)-54.9(2)° (average: 53.6°).[11a] The Cl1-Zn1-Cl2 angle is 121.3(8)°, which is close to that found in parent complex [RuClCp(PPh_3)- *μ*-dmoPTA-1κ*P*:2κ^2*N,N'*-$ZnCl_2$] (121.8(4)°).[11a] The triflate is located (Figure 2) between the C45 and F1T atoms (C45-H45B···F1T = 3.192(6) Å, H45B···F1T = 2.488(4) Å).[12,13,15]

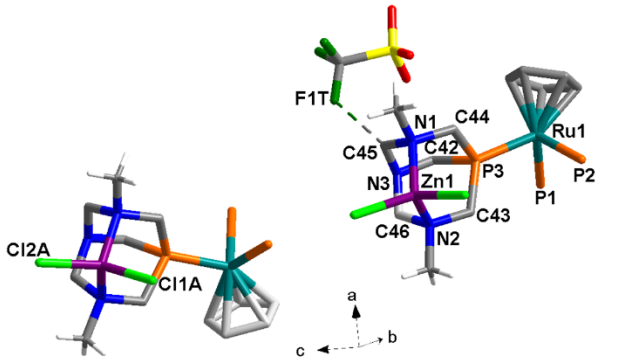

Figure 2. Perspective view and atom numbering selection of **4**, showing the two six-membered rings around the metal with a pseudo-chair conformation which form enantiomeric pairs. Dashed line represent the selected intermolecular interaction.

Table 1. GI_{50} values (μM) of **2**, **3**, **4** and **5** and cisplatin against a representative human solid tumor and, **4** and **5** versus a non-tumour cell line.[b]

	Cell line (origin)						
Entry	A549 (lung)	HBL-100 (breast)	HeLa (cervix)	SW1573 (lung)	T-47D (breast)	WiDr (colon)	BJ-hTert (fibroblasts)
2 [a]	0.29 (0.09)	0.21 (0.04)	0.17 (0.04)	0.20 (0.02)	0.25 (0.04)	0.20 (0.03)	
3 [a]	0.062 (0.019)	0.088 (0.008)	0.084 (0.022)	0.054 (0.013)	0.210 (0.05)	0.065 (0.010)	
4·	0.036 (0.019)	0.072 (0.008)	0.051 (0.022)	0.030 (0.013)	0.083 (0.05)	0.054 (0.010)	0.23 (0.02)
5·	0.14 (0.02)	0.32 (0.03)	0.19 (0.01)	0.19 (0.05)	0.33 (0.01)	0.27 (0.03)	0.35 (0.02)
cisplatin	4.9 (0.2)	1.9 (0.2)	1.8 (0.5)	2.7 (0.4)	17 (3.3)	23 (4.3)	14 (2.4)

[a] Taken from refs.[12,13]. [b] Mean of the least two independent experiments. Standard deviation in parentheses.

The structural core of **4** displays a remarkable similarity to that of **3**,[13] especially if one takes into consideration their CH_3 groups (Figure 3). In fact, the disposition of the dmoPTA ligand lays the methyl groups in different chemical environment: one of them is located in front of the Cp and the other one is near to the aromatic rings. The crystal packing diagram (Figure 4) shows weak intermolecular interactions among the molecules (C36-H36···Cl2 = 3.586(7), H36···Cl2 = 2.804(2) Å) and C–H/π interactions among adjacent phenyl–C–H groups and aromatic centroids (centroid-to-C–H distances from 3.366(5) to 3.566(6) Å), which were found larger than those found for **2**·and **3** (range from 3.183(5) to 3.470(5) Å).[12,13]

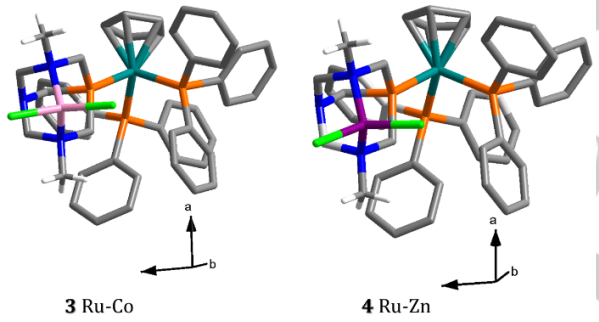

Figure 3. Equivalent enantiomeric molecules in **3** and **4**.

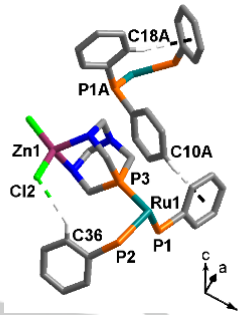

Figure 4. Perspective view and atom numbering selection of **4**, showing the significant weak interactions.

The complex **5** was characterized by elemental analysis, IR spectroscopy and NMR, supporting that the complex is constituted by a Ru atom coordinated with a piano-stool geometry to a η^5-Cp, two PPh_3 and one deprotonated dmoPTA by the P atom. The $^{31}P\{^1H\}$ NMR shows a doublet at 43.07 ppm ($^2J_{PP}$ = 38.24 Hz) due to the PPh_3 and a triplet at -7.42 ppm corresponding to the dmoPTA, which are significantly shifted to down field respecting the protonated parent complex **2** (38.44 ppm PPh_3; -13.94 ppm dmoPTA) but the coupling constant is similar (39.4 Hz). The ^1H NMR also shows the clear effect produced by the deprotonation, being the NCH_3 protons more shielded than in the protonated complex (a broad singlet at 2.04 ppm for **5**; two broad singlets at 2.35 and 2.36 ppm for **2**) but also the Cp, which is far from the deprotonation site, is shifted to upper field (4.78 ppm for **5**; 4.90 for **2**). In contrast, the $^{13}C\{^1H\}$ NMR is similar for both complexes (for example: 43.90 ppm, 44.01 ppm (**5** N**C**H_3); 43.35 ppm, 43.41 ppm (**2** N**C**H_3); 85.15 ppm (**5** Cp); 85.51 ppm (**2** Cp).

The antiproliferative activity of **4** and **5** was studied by the standard protocol (see SI) on six human solid tumour cells lines together with those for **2** and **3**[12,13] and cisplatin; which were also tested for the sake of comparison (Table 1). In order to look for selectivity, we tested also compounds **4** and **5** against the non-tumour human cell line BJ-hTert.

Complex **5** showed a similar antiproliferative activity than the starting complex **2** and therefore the protonation/deprotonation of the of the complex unit $\{[RuCpCl(PPh_3)(dmoPTA\text{-}1\kappa P)\}^+$ does not have a significant influence on its biological activity. In clear contrast and as expected, the new Ru-Zn (**4**) displays a better activity (1.2-2.5 times) than the sibling Ru-Co (**3**) and much better (26-426 times) than cisplatin. It is important to point out that complex **4** showed to be 3-8 times more active against the tumour cell lines than against the tested non-tumour cell line, indicating its large selectivity versus tumour cells. In contrast, complex **5** resulted no selective.

Complex **4**·was found to be very stable, more than the Ru-Co complex **3**, in the time needed for the antiproliferative experiments (i.e. 48 h) in a mixture of DMSO-d_6/cell-culture-medium. A very small (less than 3 %) release of PPh_3 was observed after one day which remained unvaried during one additional day. Similar experiments made in $CDCl_3$ and DMSO-d_6 showed that complex **4** is significantly more stable than complex **3** in these solvents. The dissolution of **4** in DMSO-d_6 led to the partial release of $\{ZnCl_2\}$, giving rise to the complex **5**. The reaction was not completed after 25 h and some small amount (< 5%) of released PPh_3 and complexes $\{[RuCpCl(PPh_3)(dmoPTA\text{-}1\kappa P)\}^+$,[10] and $[RuCpCl(PPh_3)\text{-}\mu\text{-}dmoPTA\text{-}1\kappa P{:}2\kappa^2 N,N'\text{-}ZnCl_2]$[11a] were observed. After 74 h under air at 40 °C, the largest signals observed by $^{31}P\{^1H\}$ NMR were still those of **4** (see SI).

Complex **4** in $CDCl_3$ slowly releases a PPh_3 to give the complex $[RuCpCl(PPh_3)\text{-}\mu\text{-}dmoPTA\text{-}1\kappa P{:}2\kappa^2 N,N'\text{-}ZnCl_2]$[11a] and the starting complex **2** (see SI), products that are obtained also with

crystalline **4** and distillate dry $CDCl_3$, which needs one chloride and one proton to occur that can only be provided by the solvent. There are references for the abstraction of Cl^- and H^+ from $CHCl_3$ and other chlorinated solvents by organometallic complexes,[16] nevertheless more experiments are needed before ensuring how proceed the transformation of **4** in $CDCl_3$ proceeds.

Conclusions

The most important conclusions are: the Ru-Zn complex **4** in solution transforms slowly and its antiproliferative activity is significantly better than those for the complexes formed by its decomposition and that for the parent Ru-Co complex **3**. Therefore, the observed larger antiproliferative activity for **4**·is due to its composition as bimetallic complex and the adequate combination of metals. The biological evaluation of $ZnCl_2$ revealed that it is not active in any of the studied cell lines. Zinc is an essential microelement in the human body and therefore, less toxic to humans than non-essential metals like platinum. It plays an important physiological role in the protein, nucleic acid as well as in the control of gene transcription, in fact is defined as an "essential trace element". Therefore, its properties as antioxidant, and its role in cancer prevention require the understanding of the complex activity-toxicity relationship.[1a,5a,17] Additionally, whilee compound **5** resulted not selective the complex **4** showed to be 3-8 times less active against a non-tumour cell line.

Works are in progress to synthesize new bis-metallic Ru-M complexes containing biologically active metals and ligands and studies targeted to understand the antiproliferative action mechanism of these family of bis-heterometal-complexes.

Experimental Section

Materials and instruments

All chemicals were reagent grade and, unless otherwise stated, were used and received by commercial suppliers. Likewise, all reactions were carried out in a pure argon atmosphere using standard Schlenk-tube techniques with freshly distilled and oxygen-free solvents. The complex $[RuCp(PPh_3)_2(HdmoPTA\text{-}1\text{-}P)](CF_3SO_3)\cdot 0.25H_2O$·(**2**·$0.25H_2O$) was synthesized using the method reported by us.[12] Elemental analysis (C,H,N) were performed on a Fisons Instruments EA 1108 elemental analyzer. Infrared spectra (KBr, Aldrich) were measured with a Thermo Nicolet Avatar 300FT-IR spectrometer. ^1H, $^{31}P\{^1H\}$ and $^{13}C\{^1H\}$ NMR spectra were recorded on a Bruker DRX300 and 500 spectrometers. Peak positions are relative to tetramethylsilane and were calibrated against the residual solvent resonance (^1H) or the deuterated solvent multiplet (^{13}C). $^{31}P\{^1H\}$ spectra were recorded on the same instrument operating at 121.49 and 282.40 MHz, respectively. Chemical shifts for $^{31}P\{^1H\}$ NMR were measured relative to external 85% H_3PO_4, it was measured with downfield values taken as positive. All NMR spectra were obtained at 25 °C.

Synthesis of $[RuCp(PPh_3)_2\text{-}\mu\text{-}dmoPTA\text{-}1\kappa P{:}2\kappa^2 N,N'\text{-}ZnCl_2]$·(OTf) (4·OTf): a) Potassium tert-butoxide (0.020 g, 0.178 mmol) was added into a solution of **2** (0.104 g, 0.090 mmol), which was synthesized as indicated in ref 12, in EtOH (10 mL) (Scheme 1). After 15 minutes at r.t. finely grounded solid $ZnCl_2$ (0.0133 g, 0.098 mmol) was added. The resulting yellow solution was kept for 30 minutes at room temperature and then reduced to 5 mL under reduced pressure. The resulting yellow solid was recrystallized in EtOH/diethyl ether (1:1), providing yellow microcrystals that were filtered and air dried. b) Complex **5** (0.100 g, 0.096 mmol) was dissolved into EtOH (5 mL) and then finely grounded solid $ZnCl_2$ (0.0133 g, 0.098 mmol) was added at room temperature (Scheme 1). After 30 minutes 5 mL of Et_2O was added into the resulting yellow solution and the mixture stirred for 5 minutes. The precipitated yellow powder was filtered, washed with Et_2O (2 x 2 mL) and dried under vacuum. Crystals yield: a) 0.049 g, 47.4 %; b) 0.069 g, 62.54 %. $S_{25°C,CHCl3}$ > 62.5 mg/mL, $S_{25°C,H2O}$ < 0.5 mg/mL, $S_{25°C,\ EtOH}$ = 10.8 mg/mL. $C_{49}H_{51}F_3Cl_2N_3O_3P_3RuZnS$ (1149.3 g mol^{-1}): Found C: 51.08; H 4.32; N 3.68; calcd. C 51.21; H 4.47; N 3.65%. IR (KBr, cm^{-1}): $\nu_{(CarH)}$ 3071, 3057; $\nu_{(CH)}$ 2961, 2915, 2861; $\delta as_{(CH)}$ 1434 (m); $\nu_{(OTf)}$ 1274, 1252, 1170, 1158; $\nu_{(C\text{-}N)}$ 1029 (m), 1071 (m); $\delta oop_{(Car\text{-}H)}$ 757 (m), 745 (m); $\delta oop_{(C=Car)}$ 690 (s). ^1H NMR (500.13 MHz, 25ºC, $CDCl_3$): δ(ppm) 2.16, 2.15 (bs+bs, NCH_3, 6H), 2.97–3.60 (m, PCH_2, 6H), 3.63–4.31 (m, NCH_2N, 4H), 4.94 (s, Cp, 5H), 6.93–7.53 (bm, aromatic, 30H). $^{13}C\{^1H\}$ NMR (125.76 MHz, 25 °C, $CDCl_3$): δ(ppm): 44.67 (s, CH_3N), 44.72 (s, CH_3N), 52.39 (d, $^1J_{PC}$ = 25.81 Hz, PCH_2NCH_3), 57.28 (d, $^1J_{PC}$ = 11.19 Hz, PCH_2NCH_3), 73.85 (s, CH_2N), 85.48 (s, Cp), 122.2, (q, $^1J_{CF}$ = 324.55 Hz, OSO_2CF_3), 129.12, 130.95, 133.46, 136.48 (m, PPh_3). $^{31}P\{^1H\}$ NMR (202.46 MHz, 25 °C, $CDCl_3$): δ(ppm) -15.10 (t, $^2J_{PP}$ = 39.15 Hz, dmPTA), 37.50 (d, $^2J_{PP}$ = 39.90 Hz, PPh_3).

Synthesis of $[RuCp(PPh_3)_2(dmoPTA\text{-}1\kappa P)]$·(OTf) (5·OTf): Potassium tert-butoxide (0.0182 g, 0.162 mmol) was added into a tetrahydrofuran (30 mL) suspension of **2** (0.1777 g, 0.155 mmol) (Scheme 1). The mixture was stirred at room temperature for 15 minutes and the solvent removed. The yellow residue was treated with $CHCl_3$ (10 mL) and the insoluble solid separated out by filtration and washed with $CHCl_3$ (2 x 2 mL). The filtered dissolution together with the washing waters were evaporated under reduced pressure and the resulting solid washed with THF/diethyl ether (1:3), filtered and dried under vacuum. Yield: 0.106 g, 67.51 %. $S_{25°C,CHCl3}$ > 15.5 mg/mL, $S_{25°C,H2O}$ < 0.5 mg/mL, $S_{25°C,\ MeOH}$ > 6.3 mg/mL. $C_{49}H_{51}F_3N_3O_3P_3RuS$ (1013.00 g mol^{-1}): Found C: 58.18; H 5.18; N 4.10; calcd. C 58.10; H 5.07; N 4.15 %. IR (KBr, cm^{-1}): $\nu_{(CarH)}$ 3080, 3055; $\nu_{(CH)}$ 2970 ,2931, 2890; $\delta as_{(CH)}$ 1435 (m); $\nu_{(OTf)}$ 1280, 1257, 1222, 1157; $\nu_{(C\text{-}N)}$ 1029 (m), 1859 (m); $\delta oop_{(Car\text{-}H)}$ 752 (m), 698 (m); $\delta oop_{(C=Car)}$ 690 (s). ^1H NMR (500.13 MHz, 25ºC, $CDCl_3$): δ(ppm) 2.04 (bs, NCH_3, 6H), 2.77–3.35 (m, PCH_2, 6H), 3.47–3.53 (m, NCH_2N, 4H), 4.78 (s, Cp, 5H), 6.97–7.03, 7.28–7.35, 7.44–7.48 (bm, aromatic, 12H, 12H, 6H). $^{13}C\{^1H\}$ NMR (125.76 MHz, 25 °C, $CDCl_3$): δ(ppm) 43.90, 44.01 (s+s, CH_3N), 55.70 (d, $^1J_{PC}$ = 28.3 Hz, PCH_2NCH_3), 74.76 (s, CH_2N), 85.15 (s, Cp), 128.57-137.14 (m, aromatic). $^{31}P\{^1H\}$ NMR (202.46 MHz, 25 °C, $CDCl_3$): δ(ppm) -7.42 (t, $^2J_{PP}$ = 38.24 Hz, dmoPTA), 43.23 (d, $^2J_{PP}$ = 38.24 Hz, PPh_3).

Single Crystal X-ray Crystallography of complex 4·OTf: A single crystal with suitable dimensions (0.03 x 0.021 x 0.017) was mounted on a glass fibber with cyanoacrylate at room temperature. Data collection was performed on a Bruker APEX-II CCD diffractometer in the range $0.952 \le 2\theta \le 26.372$. Data were collected at 100 º K using graphite-monochromatized Mo-K_α (λ = 0.71073) in the range $-13 \le h \le 9$, $-26 \le k \le 26$, $-25 \le l \le 27$. The structure was determined by direct methods and refined by least-squares procedures on F^2 (SHELX-XL) using Olex2 package.[18,19] The final geometrical calculations, the graphical manipulations and the analysis of H-bond network and other crystallographic calculations were carried out with Olex2 package.[19] The hydrogen atoms were located at the calculated positions. The chloride ligand (Cl3) was found to be disordered and refined anisotropically. One of the OTf anion of the asymmetric unit is found disordered. Crystal data and data collection details are given in Table S1. CCDC 1839217 contains the supplementary crystallographic data for this paper. These data can be obtained free of charge via the World Wide Web (or from the Cambridge Crystallographic Data Centre, 12 Union Road, Cambridge CB21EZ, UK; fax: (+44)1223-336-033 or emailing deposit@ccdc.cam.ac.uk).

Growth inhibition assays: The human solid tumor cell lines A549, HBL-100, HeLa, SW1573, T-47D and WiDr were used in this study. The human fibroblast (non- tumour) cell line BJ-hTert was used to study compound selectivity. These cell lines were a kind gift from Prof. G. J. Peters (VU Medical Center, Amsterdam, Netherlands). Cells were maintained in 25 cm^2 culture flasks in RPMI 1640 supplemented with 5% heat inactivated

fetal calf serum and 2 mM L-glutamine in a 37 °C, 5% CO_2, 95% humidified air incubator. Exponentially growing cells were trypsinized and re-suspended in antibiotic containing medium (100 units of penicillin G and 0.1 mg of streptomycin per mL). Single cell suspensions displaying >97% viability by trypan blue dye exclusion were subsequently counted. After counting, dilutions were made to give the appropriate cell densities for inoculation onto 96-well microtiter plates. Cells were inoculated in a volume of 100 µL per well at densities of 2 500 (A549, HBL-100 and HeLa) and 5 000 (SW1573, T-47D and WiDr) cells per well, based on their doubling times. Compounds were initially dissolved in DMSO at 400 times the desired final maximum test concentration. Control cells were exposed to an equivalent concentration of DMSO (0.25% v/v, negative control). Each agent was tested in triplicate at different dilutions in the range of 1–100 µM. The drug treatment was started on day 1 after plating. Drug incubation times were 48 h, after which time cells were precipitated with 25 µL ice-cold TCA (50% w/v) and fixed for 60 min at 4 °C. Then the SRB assay was performed. The optical density (OD) of each well was measured at 530 nm, using BioTek's PowerWave XS Absorbance Microplate Reader. Values were corrected for background OD from wells only containing medium.

Acknowledgements

Thanks are due to the European Commission FEDER program for co-financing the project CTQ2015-67384-R (MINECO), the Junta de Andalucía PAI-research group FQM-317 and the COST Action CM1302 (WG1, WG2). Z. M. is grateful at University of La Laguna (LL) for a predoctoral grant.

Keywords: Antiproliferation, cancer, heterometallic complexes, PTA derivatives, ruthenium.

[1] a) E. Alessio, Z. Guo, *Eur. J. Inorg. Chem.* **2017**, *2017*, 1539–1540; b) E. Alessio, *Eur. J. Inorg. Chem.* **2017**, *2017*, 1549–1560; c) P. Zhang, P.J. Sadler, *Eur. J. Inorg. Chem.* **2017**, *2017*, 1541–1548; d) I. Romero-Canelón, P.J. Sadler, *Inorg. Chem.,* **2013**, *52*, 12276−12291.

[2] J. Reedijk, *Platinum Metals Rev.,* **2008**, *52*, 2–11.

[3] a) F. Marchetti, R. Pettinari, C. Di Nicola, C. Pettinari, J. Palmucci, R. Scopelliti, T. Riedel, B. Therrien, A. Galindo, P. J. Dyson, *Dalton Trans.,* **2018**, *47*, 868–878; b) C. Gaiddon, M. Pfeffer, *Eur. J. Inorg. Chem.* **2017**, *2017*, 1639–1654; c) S. Q. Yap, C. Fei Chin, A.H. Hong Thng, Y. Yun Pang, H. Kiat Ho, W. Han Ang, *ChemMedChem.* **2017**, *12*, 300–311; d) J. Palmucci, F. Marchetti, R. Pettinari, C. Pettinari, R. Scopelliti, T. Riedel, B. Therrien, A. Galindo. P. J. Dyson, *Inorg. Chem.* **2016**, *55*, 11770−11781.

[4] a) L. Côrte-Real, R. G. Teixeira, P. Gírio, E. Comsa, A. Moreno, R. Nasr, H. Baubichon-Cortay, F. Avecilla, F. Marques, M. P. Robalo, P. Mendes, J. P. P. Ramalho, M. H. Garcia, P. Falson, A. Valente, *Inorg. Chem.* **2018**, *57*, 4629−4639; b) B.S. Murray, M.V. Babak, C.G. Hartinger, P.J. Dyson, *Coord. Chem. Rev.* **2016**, *306*, 86–114; c) W. Han Ang, A. Casini, G. Sava, P.J. Dyson, *J. Organomet. Chem.,* **2011**, *696*, 989-998; d) G. Süss-Fink, *Dalton Trans.,* **2010**, *39*, 1673–1688.

[5] a) T. Sriskandakumar, S. Behyan, A. Habtemariam, P. J. Sadler, P. Kennepohl, *Inorg. Chem.,* **2015**, *54*, 11574−11580; b) E. M. Peña-Méndez, B. González, P. Lorenzo, A. Romerosa, J. Havel, *Rapid Commun. Mass Spectrom.,* 2009; **23**, 3831–3836.

[6] N. D. Akbayeva, L. Gonsalvi, W. Oberhauser, M. Peruzzini, F. Vizza, P. Brüggeller, A. Romerosa, G. Sava, A. Bergamo, *Chem. Commun.* **2003**, 264–265.

[7] A. Romerosa, T. Campos-Malpartida, C. Lidrissi, M. Saoud, M. Serrano-Ruiz, J.A. Garrido-Cárdenas, F. García-Moroto, *Inorg. Chem.,* **2006**, *45*, 1289-1298.

[8] C. Ríos-Luci, L.G. León, A. Mena-Cruz, E. Pérez-Roth, P. Lorenzo-Luis, A. Romerosa, J.M. Padrón, *Bioorg. Med. Chem. Lett* **2011**, *21*, 4568-4571.

[9] A. Mena-Cruz, M. Serrano-Ruiz, P. Lorenzo-Luis, A. Romerosa, Á. Kathó, F. Joó, L. M. Aguilera-Sáez. *J. Mol. Catal. A-Chem.* **2016**, *411*, 27–33.

[10] A. Mena-Cruz, P. Lorenzo-Luis, A. Romerosa, M. Saoud, M., M. Serrano-Ruiz, *Inorg. Chem.* **2007**, *46*, 6120-6128.

[11] a) M. Serrano-Ruiz, L. M. Aguilera-Sáez, P. Lorenzo-Luis, J. M. Padrón, A. Romerosa, *Dalton Trans.* **2013**, 42, 11212–11219; b) A. Mena-Cruz, P. Lorenzo-Luis, V. Passarelli, A. Romerosa, M. Serrano-Ruiz, *Dalton Trans.* **2011**, *40*, 3237-3244; c) A. Mena-Cruz, P. Lorenzo-Luis, A. Romerosa, M. Serrano-Ruiz, *Inorg. Chem.,* **2008**, *47*, 2246-2248.

[12] Z. Mendoza, P. Lorenzo-Luis, M. Serrano-Ruiz, E. Martín-Batista, J.M. Padrón, F. Scalambra, A. Romerosa, *Inorg. Chem.,* **2016**, *55*, 7820−7822.

[13] Z. Mendoza, P. Lorenzo-Luis, F. Scalambra, J.M. Padrón, A. Romerosa, *Dalton Trans.,* **2017**, *46*, 8009-8012.

[14] a) S. Spreckelmeyer, C. Orvig, A. Casini, *Molecules* **2014**, *19*, 15584-15610; b) M. J. Clarke, *Coord. Chem. Rev.* **2002**, *232*, 69-93.

[15] B. González, P. Lorenzo-Luis, P. Gili, A. Romerosa, M. Serrano-Ruiz, *J. Organomet. Chem.,* **2009**, *694*, 2029–2036, and references therein.

[16] a) T. Mayer, H.-C. Böttcher, *Z. Naturforsch* **2013**, *68b*, 743 –746; b) R. P. Nair, T. H. Kim, B. J. Frost, *Organometallics* **2009**, *28*, 4681–4688; c) J. H. Park, J. H. Koh, J. Park, *Organometallics* **2001**, *20*, 1892-1894; d) I. del Río, G. van Koten, *Organometallics*, **2000,** *19,* 361-364.

[17] D. K. Dhawan, D. Chadha Vijayta, *Indian J Med Res.* **2010**, *132*, 676–682; b) S. Frassinetti, G. Bronzetti, L. Caltavuturo, M. Cini, C. Della Croce, *J Environ Pathol Tox.* **2006**, *25*, 597-610.

[18] O. V. Dolomanov, L. J. Bourhis, R. J. Gildea, J. A. K. Howard, H. Puschmann, *J. Appl. Cryst.* **2009**, *42*, 339.

[19] G. M. Sheldrick, *Acta Cryst.* **2015**, A71, 3.

Entry for the Table of Contents (Please choose one layout)

Layout 1:

COMMUNICATION

A new bi-metallic complex [RuCp(PPh$_3$)$_2$-*μ*-dmoPTA-1κP:2k^2*N,N'*-ZnCl$_2$] show 26-426 times more potent antiproliferative activity than cisplatin against a representative panel of human cancer cells.

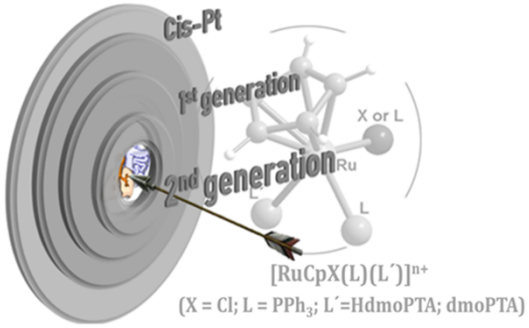

Key Topic* Antiproliferation

PhD student Zenaida Mendoza,[a] Prof. Dr. Pablo Lorenzo-Luis,[a] Dr. Franco Scalambra,[b] Prof. Dr. José M. Padrón[c] and Prof. Dr. Antonio Romerosa[b]*

Page No. – Page No.

One step up in antiproliferative activity: the Ru-Zn complex [RuCp(PPh$_3$)$_2$-*μ*-dmoPTA-1κ*P*:2k^2*N,N'*-ZnCl$_2$](CF$_3$SO$_3$)